Check for updates

Effect of the lignin type on the gas/UV barrier properties of lignin–polyethyleneimine based composite films

Asuka Yanagawa, [ID] [a] Asami Suzuki, [a] Anri Watanabe, [ID] [a] Takashi Makino, [ID] [a] Yuichiro Otsuka [ID] [b] and Kazuhiro Shikinaka [ID] ⋆[a]

In this work, the film forming abilities, gas barrier properties, and ultraviolet (UV) barrier properties of composite films composed of lignin derivatives and polyethyleneimine (PEI) were investigated. Three types of lignin derivatives were employed, namely SESC lignin (SESC) obtained by simultaneous enzymatic saccharification and comminution, along with lignosulfonate (LS) and soda lignin (Soda), which were obtained through pulping processes. All three lignin derivatives produced uniform films under appropriate conditions through the formation of polyion complexes (PICs) with PEI, which occurred *via* ionic interactions. The gas and UV barrier properties of the resulting films were tunable depending on the type of lignin derivative, the molecular weight of PEI, and the mixing ratio. Notably, the films composed of SESC and PEI exhibited excellent barrier properties while maintaining high transparency. Since these composite films can be produced in aqueous systems without the use of organic solvents, they offer potential for application in environmentally friendly packaging materials.

Introduction

Currently, the majority of chemical products are produced from fossil fuels, with approximately 8% of all fossil fuel resources being used to produce polymers.[1,2] Thus, to achieve a decarbonized society, it is necessary to break away from such resources. Consequently, the use of biomass as an alternative to fossil fuels has been increasingly explored.[3–6]

Lignin, which is the most abundant aromatic polymer in nature, is the second most prevalent natural polymer after cellulose.[7,8] Although approximately 100 million tons of lignin are produced annually, roughly 98% is discarded as a by-product of the paper industry, and only around 2% is actually utilized.[9] Furthermore, conventional lignin extraction methods (including Kraft, sulfite, alkaline, organosolv, steam explosion, and hydrolysis processes)[10] often involve high temperatures, pressures, and the use of organic solvents, resulting in a high environmental impact and degradation of the lignin structure.

To overcome these issues, our group previously reported a novel lignin extraction method, namely simultaneous enzymatic saccharification and comminution (SESC process).[11,12] This technique facilitates the isolation of polysaccharides as a sugar solution and lignin as an aqueous dispersion under

conditions that minimize the environmental impact. Additionally, composite materials incorporating a lignin derivative from the SESC process (hereafter referred to as SESC lignin), together with polymers and clays, have demonstrated effective ultraviolet (UV) absorption in a poly(vinyl alcohol) matrix,[13] as well as exhibiting gas barrier properties when combined with polymers and clays.[14] These observations suggest that such composites could exhibit gas barrier properties while retaining the UV barrier properties of lignin derivatives.

The preparation of composite films by mixing lignin derivatives and polyethyleneimine (PEI) is therefore desirable to provide films with gas barrier properties. PEI is a cationic polymer containing primary, secondary and tertiary amines, and is known to form complexes with anionic polymers, such as lignin. Thin films composed of lignin derivative and PEI have been prepared *via* a layer-by-layer (LbL) approach, and multilayered structures have been applied to bio-based coatings and nanofiltration membranes.[15] Additionally, Shi *et al.* reported that composite materials consisting of a double-hydrophilic diblock copolymer and sodium lignosulfonate, formed polyion complexes (PICs) through electrostatic attractions.[16] Such PICs effectively reduce gas permeability by densifying the structures of the composite films. The use of PICs also enables film formation *via* simple solution casting without the requirement for multiple steps, such as those employed in the conventional LbL approach, thereby providing a simpler and more practical process. However, to the best of our knowledge, the PIC-based preparation of films exhibiting gas-barrier

[a]Research Institute for Chemical Process Technology, National Institute of Advanced Industrial Science and Technology (AIST), Nigatake, 4-2-1, Miyagino-ku, Sendai 983-8551, Japan. E-mail: kaz.shikinaka@aist.go.jp

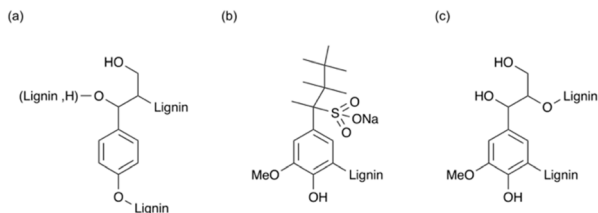*[b]Forestry and Forest Products Research Institute, Matsunosato, 1, Tsukuba 305-8687, Japan*

Fig. 1 Chemical structures of (a) SESC lignin, (b) lignosulfonate, and (c) soda lignin.

properties using lignin derivative and PEI has not yet been investigated.

The aim of the present study is therefore to prepare composite films by solution casting through the formation of PICs between lignin derivatives and PEI, and to investigate the effect of the lignin derivative type on the gas and UV barrier properties. For this purpose, PEI is mixed with three types of lignin derivatives, namely SESC lignin and two representative lignin derivatives extracted by steam cooking, *i.e.*, lignosulfonate (LS) and soda lignin (Soda) (Fig. 1). Subsequently, the effects of different lignin species and the PEI molecular weight on the resulting gas barrier properties are investigated using helium as a model gas due to its small kinetic diameter and similar permeability to hydrogen.[17] The ability of the aromatic structure of lignin to impart UV protection properties to the composite films is investigated. Such films could potentially protect polymeric materials from UV-induced degradation, rendering them suitable for use in packaging applications.

Experimental

Materials

Cryptomeria japonica (Japanese cedar) wood was harvested at the Chiyoda nursery farm of the Forestry and Forest Products Research Institute (FFPRI) in Kasumigaura City, Ibaraki, Japan. SESC lignin was extracted from this wood through SESC according to our previous work.[11] Lignosulfonate (LS; Tokyo Chemical Industry Co., Ltd, Japan) was used without further purification. Soda lignin (Soda) was extracted from Japanese cedar upon cooking with soda and anthraquinone.[18] Poly-ethyleneimines (weight average molecular weight, $M_w = 600$, 1800, and 10 000) and the polyethyleneimine solution (50 wt% in H_2O, $M_w = 70 000$) were purchased from Wako Pure Chemical Industries, Ltd, Japan and Sigma-Aldrich Co., USA, respectively. Ethanol (>99.5%, Wako Pure Chemical Industries, Ltd, Japan) was used as received without additional purification. Ultrapure water obtained from a water purification system (Milli-Q® Advantage A10® system, Millipore, Germany), was used throughout the experiments.

To obtain SESC lignin, cedar powder, an equal amount of OPTIMASH XL (containing cellulase and xylanase) and OPTI-MASH BG (containing xylanase and β-glucosidase) from DuPont™ Genencor® Science, and 100 mM phosphate buffer (pH 6.0) were processed by grinding using zirconia beads and bead milling (Labstar® LMZ015, Ashizawa Finetech Ltd, Japan)

at 50 °C under a peripheral velocity of 14.0 m s⁻¹. The inner wall of the LMZ015 instrument was covered with ceramic to prevent enzyme degradation during the process. After 2 h, the resulting mixture was subjected to centrifugation at 10 000×*g* for 30 min. The precipitate was then milled again under the same enzyme and buffer conditions. Subsequently, the slurry was subjected to centrifugation under the conditions described above, and the precipitate was washed twice with an equal volume of ultrapure water. Centrifugation was repeated once again under the same conditions to afford the brown SESC lignin as a residue.

Preparation of the composite films using PEI and the various lignin specimens

Composite films were prepared by mixing three types of lignin and four PEIs of different molecular weights in various weight ratios. As an example procedure, a 3 wt% aqueous dispersion of lignin and a 2 wt% aqueous solution of PEI were stirred for 15 min using a rotary shaker (RS-12, Sanki Seiki Co., Ltd, Japan). After this time, the two solutions were mixed and sonicated using an ultrasonic mixer (PR-1 Nano Premixer, THINKY Corp., Japan) at 140 W and 600 rpm for 30 min. Subsequently, the mixture was degassed using a planetary centrifugal mixer (ARE-250, THINKY Corp., Japan) at 2200 rpm for 5 min. The resulting mixture was cast onto a 100 μm-thick polyethylene tere-phthalate (PET) sheet and air-dried overnight at 25 °C to afford the composite film with a thickness of approximately 10 μm.

Measurement of the intermolecular interactions

To estimate the intermolecular interactions, the Fourier trans-form infrared (FTIR) spectra were recorded using an FTIR spectrometer (Nicolet iS50R, Thermo Fisher Scientific Inc., USA) equipped with an attenuated total reflectance (ATR) accessory.

Measurement of the helium gas permeability

The helium gas transmission rates of the prepared films were determined using a high-temperature compatible sample holder (GTR-10XASS, GTR TEC Corp., Japan) and high-temperature gas permeability measurement apparatus equip-ped with a helium leak detector (M-222LD, Canon Anelva Corp., Japan). Specific details regarding the measurement setup and procedure have been described previously.[19]

Measurement of the optical properties

The transmittance of each film at 200–800 nm was measured using a UV-Vis spectrophotometer (U-2910, Hitachi High-Tech Corp., Japan). The UVA and UVB transmittances were calcu-lated as the average values obtained over the 315–400 and 290–315 nm ranges (5 nm intervals), respectively, as described in the AS/NZS4399 standard.[20] The total light transmittance (Tt) and haze values were measured using a haze meter (NDH5000, Nippon Denshoku Industries Co., Ltd, Japan).

Measurement of the dispersion and microstructure

The zeta potentials and particle sizes of the lignin–PEI mixtures were measured by dynamic light scattering (DLS) using a zeta

Paper

potential and particle size analyzer (ELSZneo, Otsuka Electronics Co., Ltd, Japan) at a concentration of 0.068 w/v%. The surfaces of the composite films were observed using a digital microscope (VHX-X1, Keyence Corp., Japan).

Measurement of the durability

Accelerated weathering tests were carried out using an EYE Super Xenon Tester (XER-W83, Iwasaki Electric Co., Ltd, Japan). The composite films were subjected to accelerated weathering by irradiation in the 300–400 nm range at a total irradiance of 60 W m^{-2}, while maintaining the chamber temperature at 60 °C and the relative humidity at 50%, for a total exposure time of 240 h. The mechanical strength was evaluated by a mandrel bend test using cylindrical mandrels in accordance with ASTM D522.

Measurement of the color space

The color of the lignin-PEI films was defined based on the CIELAB ($L*a*b*$) color space, which was measured using a color spectrophotometer (CM-2600d, Konica Minolta, Inc., Japan).

Results and discussion

Film forming properties

Table 1 summarizes the film forming abilities of the composite films prepared using various lignin derivatives and PEI (hereafter referred to as the SESC-PEI, LS-PEI, and soda-PEI films). The film forming ability was evaluated based on the uniformity of each dried film. Specifically, excessive stickiness, or cracking and peeling from the PET substrate corresponded to a poor film forming ability. Thus, SESC, LS, and soda were mixed with PEI in water and cast under specific mixing conditions to produce the target films. Since the PEI raw materials were liquids and were unable to form films independently, successful film formation was attributed to the formation of PICs between lignin and PEI. For example, using SESC and PEI ($M_w = 10\,000$), films were generated across broad lignin/PEI ratios ranging

from 10 : 90 to 67 : 33, although a ratio of 10 : 90 led to a slightly viscous film due to the excess PEI. On the other hand, no film was formed at a lignin/PEI ratio of 75 : 25, where lignin was in excess. At lignin contents >75 wt%, a precipitated formed during mixing, preventing uniform dispersion. This was attributed to microparticle aggregation/precipitation, which was caused by an increased anion ratio within the PICs formed between the anionic lignin[21] and the cationic PEI[22] (Fig. 2C1, c1). In the presence of excess lignin, the limited amount of PEI restricts the formation of PICs. Consequently, the generated PICs grow into secondary complexes by adsorbing excess lignin derivative from the solution, leading to the formation of microparticles.[23] No film formation was observed when the low-molecular-weight PEI ($M_w = 600$ or 1800) was employed at a lignin/PEI ratio of 17 : 83 for any of the lignin types. This was attributed to the insufficient interactions between the lignin derivative and the short PEI chains, as well as the high content of the liquid PEI. In the cases of SESC and soda systems, film formation became possible when using the higher-molecular-weight PEI ($M_w = 10\,000$ or 70 000). For these lignin derivatives, even under excess PEI conditions, film formation was possible due to the weak hydrogen bonding of the lignin –OH groups without aggregation. On the other hand, when LS was used, film formation was not observed at a lignin/PEI ratio of 17 : 83, whereas it became possible at a 50 : 50 ratio. At lignin/PEI ratios of 17 : 83 and 50 : 50, the particle sizes in the dispersions were determined to be 4.0 and 4.3 nm (Fig. 2A2, a2), respectively. Although the particle size was maintained even after film formation using a lignin/PEI ratio of 17 : 83, a ratio of 50 : 50 produced an increased in particle size (several tens to hundreds of nanometers), indicating the formation of PICs (Fig. 2B2, b2). Since LS possesses strong anionic character due to its sulfonic acid ($-SO_3^-$) groups, it is expected to interact strongly with PEI via electrostatic interactions. However, the high hydrophilicity of LS stabilizes its hydrated state in the dispersion, thereby suppressing the growth of PICs. Using a lignin/PEI ratio of 50 : 50, the charge balance between the anionic and cationic groups became more favorable for PIC formation compared with that achieved using a 17 : 83 ratio. Moreover, water removal during the film formation process promoted the generation of PICs, which ultimately enabled successful film formation. The formation of PICs was further supported by FTIR analysis (Fig. S1). In all composite materials, peak broadening was observed in the range of 3300–3400 cm^{-1} was observed. This peak was attributed to the O–H stretching vibrations of the phenolic hydroxyl groups in lignin derivatives, and its broadening extended to the N–H stretching vibration of PEI at 3275 cm^{-1}. Similarly, the characteristic peaks of PEI assigned to N–H scissoring bending vibrations (1584 and 1457 cm^{-1}). It seems that C–N stretching vibrations of the aliphatic amines (1105 and 1044 cm^{-1}) exhibited decreasing intensity or shifting peak. These spectral changes collectively suggest the presence of interactions between the phenolic hydroxyl groups in lignin derivatives and the amine groups of PEI. The zeta potentials of the lignin derivatives were −26.50, −33.90, and −33.29 mV for SESC, LS, and soda lignin, respectively, reflecting differences in their anionic character arising

Table 1 Film forming abilities of the lignin-PEI films. ○: The lignin-PEI film was successfully formed. ✗: no lignin-PEI film was formed. —: not tested

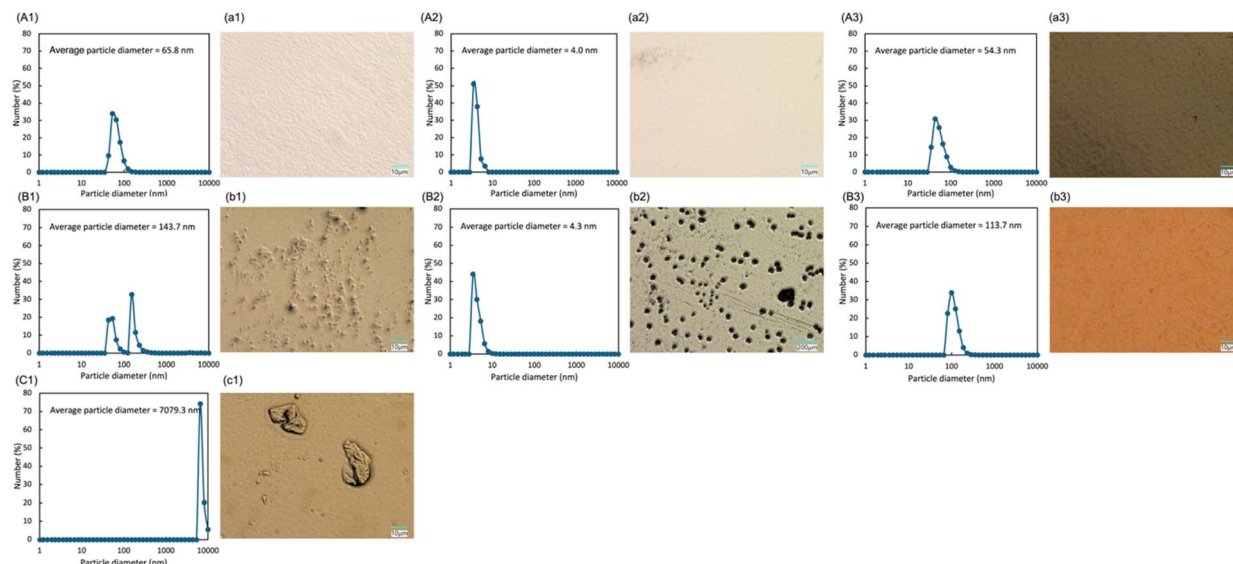| Lignin	Lignin/PEI ratio	PEI M_w			
		600	1800	10 000	70 000
SESC	0/100	—	—	✗	—
	10/90	—	—	○	—
	17/83	✗	✗	○	○
	25/75	—	—	○	—
	33/67	—	—	○	—
	50/50	○	○	○	○
	67/33	—	—	○	—
	75/25	—	—	✗	—
LS	17/83	✗	✗	✗	✗
	50/50	○	○	○	○
Soda	17/83	✗	✗	○	○
	50/50	○	○	○	○

Fig. 2 Particle size determination based on the DLS and the digital microscopy images recorded for a PEI M_w of 10 000. Numbers 1–3 represent SESC, LS, and soda, respectively. Panels (A–C) indicate the particle size determination results, while panels (a–c) shows the corresponding digital microscopy images recorded at lignin/PEI ratios of 17 : 83, 50 : 50, and 75 : 25, respectively.

from the contents and acidities of their acidic functional groups (Table S1). The zeta potentials of lignin/PEI dispersions ranged from −2.69 to 1.54 mV, suggesting that charge neutralization occurred in the lignin/PEI systems. However, no clear correlation with lignin type or mixing ratio was observed. This is likely because changes in lignin species and composition induce the formation of insoluble fractions and aggregates, so that the measured zeta potentials do not simply reflect the surface charge of dispersed particles.

Helium gas permeability

The helium gas permeability was subsequently measured for each SESC-PEI film (Table 2). When the M_w of PEI was fixed at 10 000, the lowest helium gas permeability (1.7×10^{-16} mol·m m^{-2} s^{-1} Pa^{-1}) was observed at a lignin/PEI ratio of 17 : 83.

Notably, this was the lowest helium gas permeability obtained in the current study, suggesting that the charge balance

at this ratio favors PIC formation to the greatest extent, leading to a high density and a continuous PIC structure that effectively suppressed gas permeation. This value is also lower than those of the uncoated PET sheet (5.4×10^{-16} mol·m m^{-2} s^{-1} Pa^{-1}) and those of typical polymeric membranes,[24] indicating that the SESC-PEI film provided a superior barrier performance. However, this value was higher than that reported for a composite membrane based on clay and modified lignin derivative,[25] while also being higher than that of a clay/SESC combination.[14] This difference in permeability was attributed to variations in the membrane structure. In previous studies, low permeability was achieved through the formation of an ordered layered structure by clay. In contrast, the membrane fabricated *via* PIC in this study does not exhibit a fully ordered layered structure, likely accounting for its relatively higher gas permeability. Based on these results, the lignin/PEI ratio was fixed at 50 : 50 and the M_w of PEI was varied. Consequently, the lowest gas permeability (1.9×10^{-16} mol·m m^{-2} s^{-1} Pa^{-1}) was observed for a PEI M_w of 10 000. In the case of low-molecular-weight PEI ($M_w = 600$ or 1800), PIC formation was limited due to insufficient interactions with lignin, resulting in a reduced gas barrier performance.[26] Conversely, when the M_w of PEI reached 70 000, numerous large aggregates were visible on the film surface (Fig. S2). This caused the film to lose its uniformity, preventing the formation of a continuous structure, and ultimately reducing the gas barrier performance.

Optical properties

Table 3 lists the film thicknesses, UVA and UVB transmittances, total light transmittances (Tt), and haze values of the lignin-PEI films. Additionally, as shown in Fig. 3a, the SESC-PEI films exhibited both excellent UV barrier properties and high transparency. The SESC-based film exhibited a Tt of approximately

Table 2 Helium gas permeabilities of the SESC-PEI films

PEI M_w	Lignin/PEI ratio	He permeability ($\times 10^{-16}$ mol m m^{-2} s^{-1} Pa^{-1})
600	50/50	4.6
1800	50/50	5.5
10 000	10/90	2.5
	17/83	1.7
	25/75	2.4
	33/67	3.4
	50/50	1.9
	67/33	5.1
70 000	17/83	3.2
	50/50	4.8

Table 3 Optical properties of the lignin-PEI films

Lignin	PEI M_w	Lignin/PEI ratio	Film thickness (μm)	UVA transmittance (%)	UVB transmittance (%)	Tt (%)	Haze value (%)
SESC	600	50/50	13	9.0	0.10	81	31
	1800	50/50	10	9.0	0.10	80	25
	10 000	10/90	11	57	1.0	89	1.8
		17/83	6	49	0.60	89	4.0
		25/75	18	23	0.13	87	3.6
		33/67	9	31	0.23	79	3.3
		50/50	12	15	0.10	83	1.5
		67/33	8	10	0.10	80	7.7
	70 000	17/83	8	8.0	0.32	85	2.0
		50/50	15	11	0.10	83	2.8
LS	600	50/50	6	20	0.18	85	9.8
	1800	50/50	7	21	0.22	85	11
	10 000	50/50	9	29	0.03	82	6.1
	70 000	50/50	8	33	0.38	82	4.9
Soda	600	50/50	10	0.2	0.17	51	5.6
	1800	50/50	13	9.0	0.18	49	30
	10 000	50/50	10	0.10	0.17	31	1.5
	70 000	50/50	11	0.10	0	28	1.2

80%. While films incorporating PEIs with M_w of 600 or 1800 showed slightly elevated haze values, the haze remained comparable (±10%) to those obtained with PEI M_w values of 10 000 and 70 000. Using PEI with a M_w of 10 000 in combination with a lignin/PEI ratio of 50 : 50, the resulting film exhibited a UVA transmittance of 15%, UVB transmittance of 0.10%, Tt of 83%, and haze value of 1.5%. These results indicate that the film demonstrated efficient UV protection while a maintaining high transparency. No significant change in the UV protection property was observed upon variation in the PEI M_w. In contrast, the films prepared using a low lignin content (10–33%) exhibited diminished UV shielding performances. In particular, the UVA transmittance reached 57% for a lignin/PEI ratio of 10 : 90, indicating a significant reduction in its protection properties due to the reduced lignin content. With regard to the LS-PEI films, Fig. 3b shows that these films exhibit a slightly yellowish appearance compared with the SESC-PEI films, although no significant differences were observed in their Tt and haze values. In the case of the LS-PEI films, the UVA transmittance was higher than those exhibited by the SESC-PEI films, and a high haze value of 6.1% was observed for a lignin/ PEI ratio of 50 : 50 and a PEI M_w of 10 000. Moreover, the LS-PEI films exhibited higher UV transmittance characteristics

compared with the corresponding SESC-PEI films. This can be attributed to the strong interactions between PEI and the highly polar sulfonic acid groups of LS, which promote lignin aggregation and generate a heterogeneous microstructure. This can be clearly observed in Fig. 2b2, where significantly larger particles and aggregates are present. These observations clearly contrast with the SESC-PEI films shown in Fig. 2b1. Moreover, the absorbance of SESC lignin alone was higher than that of LS lignin alone (Fig. S3), which likely contributed to the reduced UV protection properties observed for the LS-PEI films. Notably, the soda-PEI films demonstrated the lowest UV transmittance values, which seemingly indicates a superior performance. However, since soda is essentially dark in color (Fig. 3c) and possesses a low dispersibility, the soda-PEI films exhibit a dark brown color with a poor transparency. Consequently, they absorb a broad range of light (Fig. S4), not only in the UV region, but also in the visible range, ultimately leading to a decrease in the Tt. Furthermore, the durability of the lignin-PEI films was evaluated using accelerated weathering tests (Table S2). A comparison of color differences before and after the weathering test showed that the b^* value increased for all samples, confirming yellowing of the films. As a result, a decrease in UVA transmittance was observed, particularly for the SESC and LS, leading to enhanced UVA shielding performance. The minimum bending radius determined by the mandrel test was less than 1 mm for SESC and soda, and 2 mm for LS, and these values remained unchanged before and after the light-resistance test.

Conclusions

In this study, composite films exhibiting gas and UV barrier properties were prepared using three different lignin derivatives in combination with PEI. Their film forming abilities, gas barrier permeabilities, and UV barrier properties were
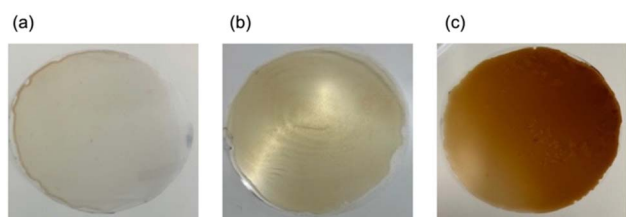

Fig. 3 Representative photographic images of the lignin-PEI films prepared from (a) SESC, (b) LS, and (c) soda. A lignin/PEI ratio of 50 : 50 was used in each case.

evaluated. The type of lignin derivative, the molecular weight of PEI, and the mixing ratio significantly influenced PIC formation. Specifically, it was found that the SESC-PEI films formed PICs with PEI due to the moderately anionic character of the lignin –OH groups, resulting in uniform film formation over a wide range of conditions. These films demonstrated high barrier properties against both helium gas and UV irradiation while retaining high transparency. In contrast, the LS-PEI films exhibited visible aggregation on the film surface due to the strong anionic character and high hydrophilicity of the LS–SO_3^- groups, which led to increased UV transmittance. Moreover, although the soda-PEI films demonstrated strong UV absorption capabilities, their poor transparency leads to limitations regarding their potential applications. Importantly, the composite films presented in this study can be easily fabricated from lignin biomass without the use of organic solvents, thereby promoting both reduced environmental impact and the high-value utilization of renewable resources. Future work will focus on enhancing the film durability from the viewpoint of practical applications, including food packaging.

Author contributions

Asuka Yanagawa: data curation, investigation, visualization, writing – original draft. Asami Suzuki: data curation, investigation. Anri Watanabe: writing – review & editing. Takashi Makino: supervision, writing – review & editing. Yuichiro Otsuka: resources. Kazuhiro Shikinaka: conceptualization, funding acquisition, project administration, supervision, writing – review & editing.

Conflicts of interest

There are no conflicts to declare.

Data availability

The data supporting this study are available in the published article and in its supplementary information (SI). Supplementary information: which includes the results of FTIR spectra, zeta potentials, digital microscopy images, UV-vis adsorption/transmittance spectra, CIELAB ($L*a*b*$) color spaces, and mandrel bend radii. See DOI: https://doi.org/10.1039/d5ra07628e.

Acknowledgements

Notes and references

1 J. Hopewell, R. Dvorak and E. Kosior, *Philos. Trans. R. Soc. B*, 2009, **364**, 2115.

2 Y. Zhu, C. Romain and C. Williams, *Nature*, 2016, **540**, 354.

3 D. Mignogna, M. Szabó, P. Ceci and P. Avino, *Sustainability*, 2024, **16**, 1123.

4 G. Coppola, M. T. Gaudio, C. G. Lopresto, V. Calabrò, S. Curcio and S. Chakraborty, *Earth Syst. Environ.*, 2021, **5**, 231.

5 M. Fazeli, J. P. Florez and R. A. Simão, *Composites B*, 2019, **163**, 207.

6 T. Nuge, M. Fazeli and H. Baniasadi, *Int. J. Biol. Macromol.*, 2024, **275**, 133480.

7 B. Zhang, G. Qiang, K. Barta and Z. Sun, *Innov. Mater.*, 2024, **2**, 100062.

8 H. Erdtman, *Lignins: Occurrence, Formation, Structure and Reactions*, ed. K. V. Sarkanen and C. H. Ludwig, Wiley Interscience, New York, 1971.

9 D. Bajwa, G. Pourhashem, A. Ullah and S. Bajwa, *Ind. Crops Prod.*, 2019, **139**, 111.

10 R. Saadan, C. H. Alaoui, A. Ihammi, M. Chigr and A. Fatimi, *Environ. Earth Sci. Proc.*, 2024, **31**, 3.

11 K. Shikinaka, Y. Otsuka, R. R. Navarro, M. Nakamura, T. Shimokawa, M. Nojiri, R. Tanigawa and K. Shigehara, *Green Chem.*, 2016, **18**, 5962.

12 R. Navarro, Y. Otsuka, M. Nojiri, S. Ishizuka, M. Nakamura, K. Shikinaka, K. Matsuo, K. Sasaki, K. Kimbara, Y. Nakashimada and J. Kato, *BMC Biotechnol.*, 2018, **18**, 45.

13 K. Shikinaka, M. Nakamura and Y. Otsuka, *Polymers*, 2020, **190**, 122254.

14 K. Shikinaka, A. Suzuki and Y. Otsuka, *RSC Adv.*, 2021, **11**, 23385.

15 A. Abbadessa, I. Dogaris, S. Farahani, M. Reid, H. Rautkoski, U. Holopainen-Mantila, P. Oinonen and G. Henriksson, *Prog. Org. Coat.*, 2023, **182**, 123.

16 N. Shi, Y. Ding, D. Wang, X. Hu, L. Li, C. Dai and D. Liu, *Int. J. Biol. Macromol.*, 2021, **187**, 722.

17 J. Humpenoder, *Cryogenics*, 1998, **38**, 143.

18 T. Ikeda and K. Magara, *J. Wood Chem. Technol.*, 2015, **35**, 167.

19 T. Aizawa, M. Kubota and T. Ebina, *Clay Sci.*, 2023, **27**, 7.

20 Standards Australia/Standards New Zealand, *Sun protective clothing – evaluation and classification*, AS/NZS 4399:2017, 2017, available at: https://www.standards.govt.nz/shop/asnzs-43992017, accessed 29 September 2025.

21 A. Suzuki, Y. Otsuka and K. Shikinaka, *Front. Bioeng. Biotechnol.*, 2022, **10**, 1001.

22 P. Barick, B. Saha, R. Mitra and S. Joshi, *Ceram. Int.*, 2015, **41**, 4289.

23 J. Gao, Q. Zhan, Z. Tang and Y. Huang, *Macromol. Rapid Commun.*, 2022, **43**, 2100567.

24 C. Scholes and U. Ghosh, *Membranes*, 2017, **7**, 12.

25 A. Suzuki, R. Ishii, H. Yoshida, T. Ebina, T. T. Nge and T. Yamada, *Clay Sci.*, 2018, **22**, 71.

26 J. M. Lagaron, R. Catalá and R. Gavara, *Mater. Sci. Technol.*, 2004, **20**, 1.